On the Machinability of Medium Density Fiberboard by Drilling

Krzysztof Szwajka [a,*] and Tomasz Trzepiecinski [b]

Machinability is one of the most important technological properties in the machining process. The machinability index is a numerical value that shows the degree of difficulty or ease with which a material can be machined. The research described herein consisted of drilling blind holes in a medium density fibreboard (MDF) using a cemented carbide tool. Different cutting speeds (v_c) and feeds (f_n) were used in the tests. The goal was to determine the value of the axial force (F_f), the cutting torque (M_c), and the chip thickness. To analyse signals involving axial force and cutting torque, a methodology for determining the average values of these signals was proposed to avoid random changes in signal values. The results obtained were used to determine the MDF machinability index in the drilling process based on the measurement of the axial force, cutting moment, and shear angle of the chips. The results obtained showed that the machinability index based on the adopted criteria is constant for a given workpiece and does not depend on the cutting parameters.

Keywords: Drilling; Cutting force; Shear angle; Medium density fiberboard (MDF)

*Contact information: a: Rzeszow University of Technology, Faculty of Mechanical Engineering and Technology, Kwiatkowskiego 4, 37-450 Stalowa Wola, Poland; b: Rzeszow University of Technology, Faculty of Mechanical Engineering and Aeronautics, al. Powst. Warszawy 8, 35-959 Rzeszów, Poland; * Corresponding author: kszwajka@prz.edu.pl*

INTRODUCTION

Medium density fiberboard (MDF) was commercially produced for the first time in the late 1960s with the intention of competing with particleboard (Clark 1991). Due to their better machinability, dimensional stability, and surface characteristics, MDFs compete with both wood-composite materials and solid wood. Currently, MDFs are mainly used in the production of furniture (Irle and Loxton 1996; Chapman 1998; Sun and Hammett 1999; Szwajka and Trzepieciński 2017). MDFs are usually covered with wood veneer or plastic laminate to simulate the appearance of a solid wood product. For the applications cited, the workability of the MDFs is determined by the quality of the surface machined (Penman *et al.* 1993; Szwajka and Trzepieciński 2016), which largely depends on the degree of tool wear and the mechanism of chip formation (Bhattacharyya *et al.* 1993). When parameters such as surface quality, tool wear, chip formation mechanism, and machining forces are discussed in relation to the workpiece material, it is generally referred to as the investigation of the "machinability" of the material. Various studies have elucidated MDF cutting characteristics (Dippon *et al*. 2000; Engin *et al*. 2000; Costes and Larricq 2002; Gordon and Hillery 2003), which were mainly focused on measuring cutting forces and friction on the cutting tool using conventional metal cutting theories. The formation of chips was not mentioned.

Lin *et al*. (2006) described the machinability of MDFs. They used a digital camera to record chip deformation occurring in front of the tool tip and a scanning electron

microscope (SEM) for additional analysis of the machined surface. The cited study showed that differences in fiberboard density are closely related to its machinability.

Orthogonal cutting is a form of machining in which the straight cutting edge is perpendicular to the direction of the relative tool movement and is a basic method in the cutting process (Koch 1964). Dippon *et al*. (2000) presented a mechanical analysis of MDF orthogonal cutting. This investigation adopted the Coulomb friction model on both surfaces of the cutting tool to predict the coefficient of friction on the rake face and tool flank. The cutting forces were expressed as a function of tool geometry, chip thickness, and constant cutting speed. Costes and Larricq (2002) estimated the distribution of stresses on the tool's rake face in the MDF orthogonal cutting process.

Davim *et al.* (2007) conducted investigations to determine the relationship between cutting parameters and delamination of the chipboard at the hole entry and exit during drilling of medium-density fibreboard (MDF). An important role was found for the cutting speed with respect to the evolution of the delamination factor as a function of the material removal rate (MRR). The study of Davim *et al.* (2008) investigated the parametric interaction between cutting speed and feed rate on the delamination factor at entry and exit of the holes in drilling of MDF. Aguilera *et al.* (2000) found that high density and low chip thickness produce optimal levels of surface roughness in machining of MDF panels.

Concerning the evaluation of delamination around the hole, there are reports (Davim and Reis 2003; Feito *et al.* 2014) where delamination factors have been used based on the measurement of the maximum diameter of observed delamination, or an area of delamination has been defined. Recently, however, certain workers increasingly use the dimensionless factor to evaluate delamination. Palanikumar *et al.* (2009) investigated the delamination in drilling of MDF and observed that the delamination can be reduced at low feed rates. Prakash *et al.* (2009) performed drilling experiments using the Taguchi technique and found that the feed rate and diameter were the most dominant factors that affect the surface quality. Prakash and Palanikumar (2011) found that the increase in drill diameter increases the delamination. Valarmathi and Palanikumar (2011) performed drilling experiments on laminated MDF panels to minimize the delamination and found that thrust force developed in drilling can be reduced with high spindle speed and low feed rate. A similar dependence was confirmed by Valarmathi *et al.* (2013b). The results showed that the most dominant factors that influence the delamination are the feed rate, followed by the drill diameter. Valarmathi *et al.* (2013a) measured and analysed the cutting conditions that influence the thrust force in drilling of particleboard panels. The parameters considered were spindle speed, feed rate, and point angle. The results showed that high spindle speed with low feed rate combination minimizes the thrust force in drilling of pre-laminated particleboard panels. Valarmathi *et al.* (2013c) conducted drilling experiments on plain and laminated MDF panels using drills of 10 mm diameter with different point angles and developed a model to evaluate the effect of drilling parameters on thrust force. They found that high spindle speed and low feed rate are the preferable cutting conditions to reduce the thrust force in drilling of MDF panels. Gaitonde *et al.* (2008a,b) studied the influence of machining conditions on thrust force and concluded that the feed rate followed by spindle speed were the most significant factors in minimising the thrust force value in drilling MDF panels.

There are several studies of the effect of drill geometry on the processing parameters and delamination of particleboard in drilling operations. Ispas and Răcășan (2017) analysed the influence of the drill tip angle and feed speed on the processing quality evaluated by the size of delamination at the entrance side and exit side of the hole. The

influence of the feed rate and tool geometry was assessed in terms of a non-dimensional quality parameter. It was found that the delamination increased with the increase of the tooth bite (feed rate) for all drill geometry analysed. Ispas *et al.* (2014) analysed the variation of the torque, thrust force and surface delamination with the drill tip angle and feed per tooth at drilling prelaminated particleboard. They found that a low feed rate generally minimizes both the thrust force, the drilling torque, and delamination. However, a small tip angle generally minimizes the delamination and the thrust force. In other work, Ispas and Răcăşan (2015) measured and analysed the influence of both the kinematic and geometric parameters on the dynamic parameters at drilling with helical drills. It was found that a low feed rate generally minimizes both the thrust force and drilling torque.

Cutting forces and surface roughness are two important issues in the machining of wood-based materials that reflect its susceptibility to material processing. Cutting forces have a direct effect on energy consumption, tool wear, heat generation, and the quality of the surface being machined (Marchal *et al*. 2009; Wyeth *et al*. 2009; Guo *et al*. 2014; Szwajka and Trzepieciński 2017). According to Jemielniak (1998), the most important machinability criteria are tool durability, the quality of the surface machined, cutting resistance, and the shape and dimensions of the chips. In the case of drilling with small diameter drills, cutting forces are a very important machinability criterion due to the danger of exceeding the critical value, which leads to drill cracking. This article is devoted to analysis of machinability by means of axial force, cutting moment, and shear chip angle simultaneously when drilling MDF. The aim of this study was to define a machinability index based on the link between axial force, cutting torque, and shear chip angle simultaneously when drilling MDF.

EXPERIMENTAL

Materials

A commercial MDF board with a thickness of 18 mm was used as the workpiece. The mechanical and physical analyses were carried out according to the EN 310 (1994) and EN 323 (1999) standards. The results are presented in Table 1. Using a scanning electron microscope (TESCAN, MIRA3, Brno, Czech Republic) with a TESCAN EDS attachment (Fig. 1a), a microphotograph of a spectral analysis was produced depicting the elements making up the test material (Fig. 1).

Table 1. Selected Mechanical and Physical Properties of MDF

Parameter	Density (kg/m^3)	Moisture Content (%)	Bending Strength (N/mm^2)	Elasticity Modulus (N/mm^2)
MDF	742	7.2	38	2530
Standard method	EN 323 (1999)	EN 322 (1999)	EN 310 (1994)	EN 310 (1994)

Based on previous reports and industrial applications, an arbor drill with a diameter of ϕ = 9.3 mm was used as the cutting tool. The blades were made of cemented carbide (grade P15) with a cutting edge angle of κ_r = 90° and rake face angle of γ_o = 15° (Fig. 2).

(a) (b) (c)

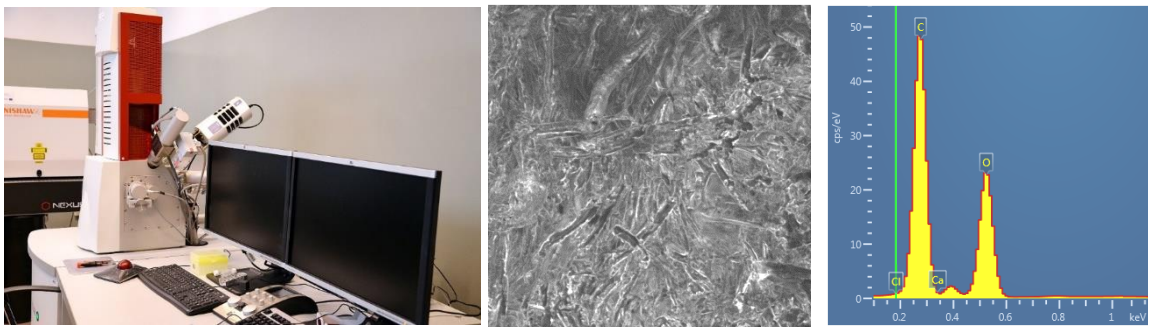

Fig. 1. (a) Scanning electron microscope, (b) a microphotograph, and (c) an EDS spectrum of MDF

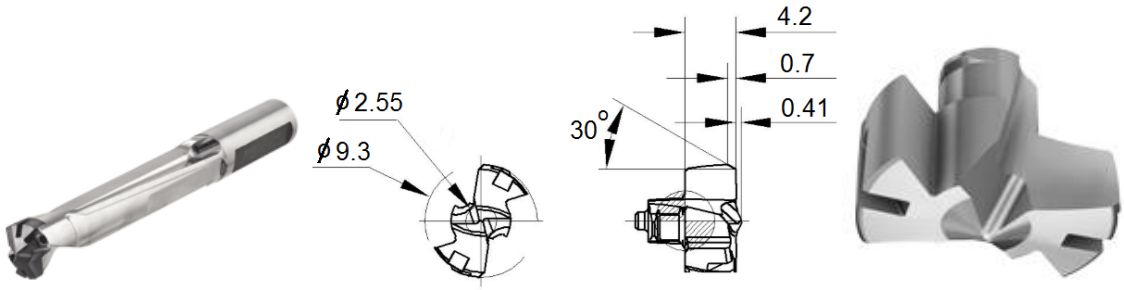

Fig. 2. Cutting tool: Shank ISCAR (DCNS 090-027-090B-3D) and blade FPC 093 IC908

Methods

Blind holes were drilled in MDF elements with the dimensions 130 × 30 × 18 mm (Fig. 3a). The values of machining parameters (F_f and M_c) were measured using the KISTLER type 9345B2 piezoelectric industrial sensor (Winterthur, Switzerland). The signals from the sensor were recorded on a personal computer (PC) disk in digital form *via* an analogue-to-digital National Instruments PCI-6034E converter (Austin, TX, USA).

The sampling rate of F_f and M_c signals during the experiments was 50 kHz per channel. The measurement resolution of the card was 16-bit. Figure 3b shows a diagrammatic representation of the measurement method used in the tests. After each hole was drilled, the thickness of the obtained chip was measured. These measurements were carried out on a Mitutoyo TM microscope (Kawasaki, Japan) equipped with a digital camera.

(a) (b)

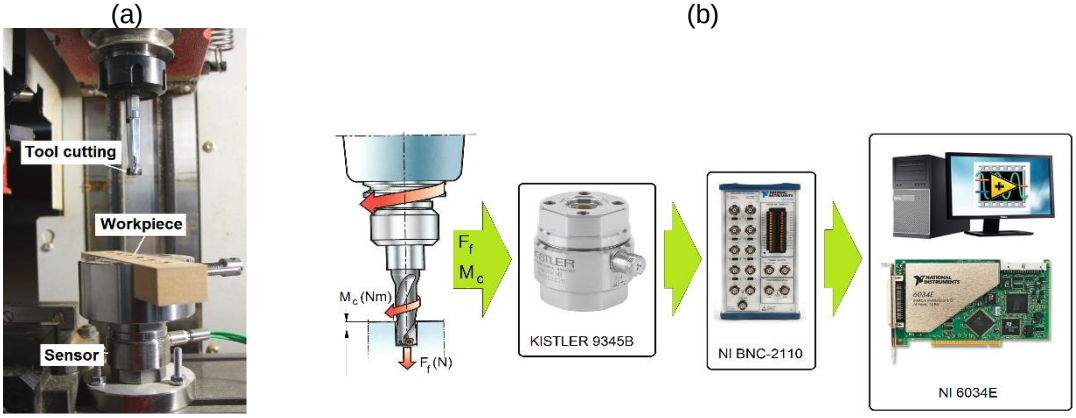

Fig. 3. (a) Experimental setup and (b) research method

During the tests, a series of holes were made for the sets of cutting parameters adopted. Four cutting speeds (v_c) were used in the tests conducted: 0.24, 0.48, 0.73, and 0.97 m/s. For each cutting speed five feed values f_n were adopted: 0.1, 0.2, 0.3, 0.4, and 0.5 mm/rev. The tests for each set of parameters were repeated three times.

RESULTS AND DISCUSSION

Thrust Force and Cutting Torque

To analyse the recorded F_f and M_c signals, a computer program was prepared in the LabView programming language manufactured by National Instruments (Austin, TX, USA). The program allowed for the determination, in selected time intervals, of the mean values of the registered axial force and cutting torque signals. The proposed method of machine cutting detection is shown in Fig. 4. The detection of machine cutting is based on the axial force signal F_f and the cutting torque M_c. After a time interval of 50 ms, and after receiving the signal 'start of feed' from the machine control system, the offset of the signal was removed. For this purpose, a standard deviation (σ_0) and an average value (S_{ave}) are determined for the signal coming from a signal fragment sensor with a specified time interval of 100 ms. The average value of the S_{ave} signal was subtracted from the total signal as an offset, so when the drill was operated in the air the signal should oscillate around approximately zero. The standard deviation calculated during the removal of the offset -σ_0, denoted here as σ_0 (F_f) and σ_0 (M_c), is a measure of signal interference, which may be dependent on spindle rotational speed, feed, *etc*. Therefore, it can be used to determine the threshold value for cutting detection. After removing the offset, the actual detection of machining begins. From a signal period of 5 ms, S_f and σ_c were determined, where S_f is a low-pass 2nd order Butterworth filtered signal with a cutoff frequency of 1 kHz, and σ_c is the standard deviation of this signal. The S_f measurement is the most effective when there is an absence of signal drift. The start of cutting is recognized if $S_f > 5$ or $\sigma_c > 3\sigma_o$ for any of the signals above 25 ms. In the example shown in Fig. 4a, the threshold transition appeared at 0.128 s. In the case of the feed force standard deviation, cutting was detected at 0.135 s (Fig. 4b). The end of cutting is recognised when the signal measures fall below the assumed threshold which was determined in the recognition at the start of cutting. The multipliers, 5 for the filtered signal S_f and 3 for the signal's standard deviation σ_c, were determined on the basis of the authors' own experience.

After determining the beginning of cutting, the signal was segmented, which consists of dividing the signal into equal time intervals during analysis. From such intervals called segments, the average value of the signals was generated. The program operation involved the automatic determination of the recorded signal value in strictly defined time periods. The signal was divided into equal time fragments in order to prepare it for analysis. The average signal value was generated from such time fragments. Before it was possible to carry out these procedures, it was necessary to select those signal fragments that will provide the best representation of the signal value during processing. Fragments of the stable (invariability) signal are the most suitable. This allows one to avoid random changes in the signal. The method of assessing the invariability of the F_L signal is presented in Fig. 5 and is described by Eq. 1,

$$F_L = \left| \frac{MS(t_{i-1})}{MS(t_i)} - 1 \right| + \left| \frac{MS(t_{i+1})}{MS(t_i)} - 1 \right| \quad (1)$$

where MS (t_{i-1}) is a measure of the signal for time t_{i-1}, and MS (t_{i+1}) is a measure of the signal for time t_{i+1}. A lower value for the F_L signal indicated that the segment was more suitable for determining the signal value.

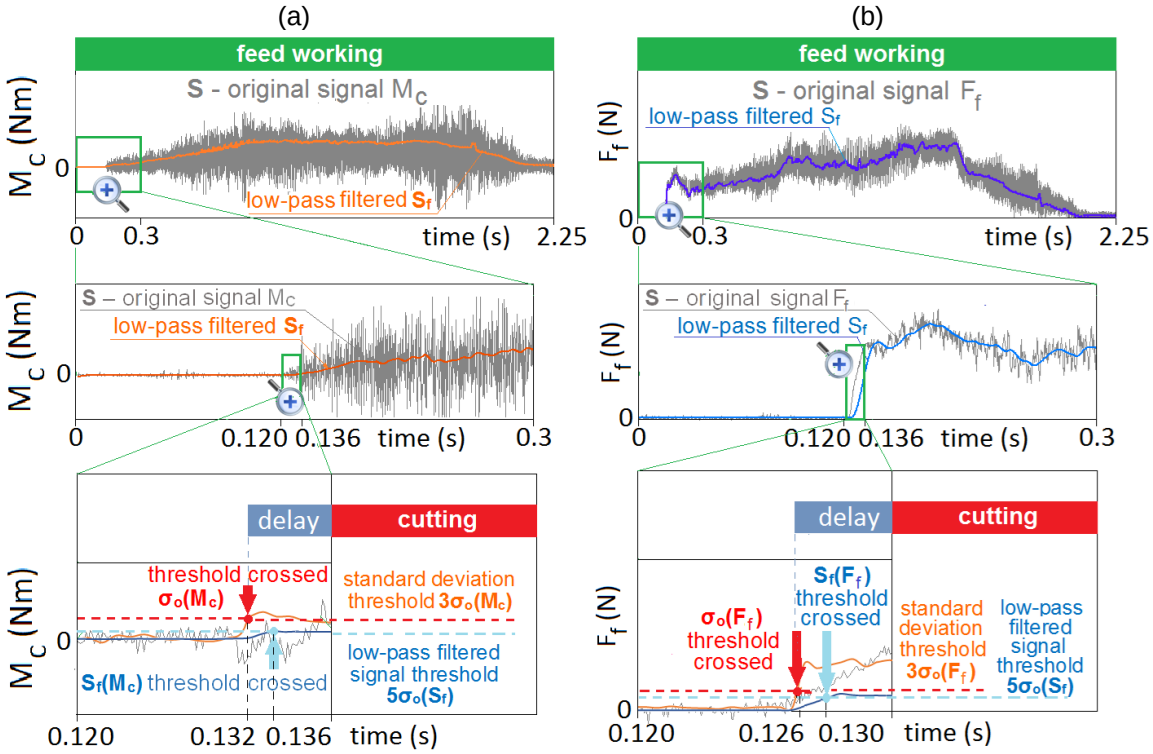

Fig. 4. Methodology for determining the beginning of cutting with regard to M_c (a) and F_f (b) signals

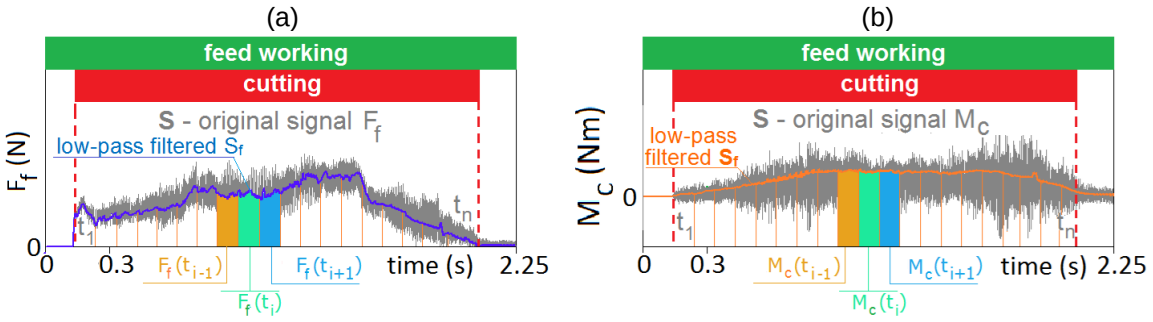

Fig. 5. Methodology for the determining the F_f (a) and M_c (b) signal values

To determine the best signal fragments for the average value evaluation from each recorded signal (during the machining of one hole), the signal segments with the best rating were selected. The methodology is shown in Fig. 5. This procedure was carried out for all recorded signals received for each of the holes drilled. The final selection consists of the selection of such signal fragments (in the same time interval) and for which the invariability of F_L is the smallest.

Figure 6 shows the variation of axial force (F_f) and cutting torque (M_c) in relation to the value of uncut chip thickness and cutting speed. Both the value of the axial force and the cutting torque increased with uncut chip thickness. A significant effect of cutting speed was observed on the axial force value.

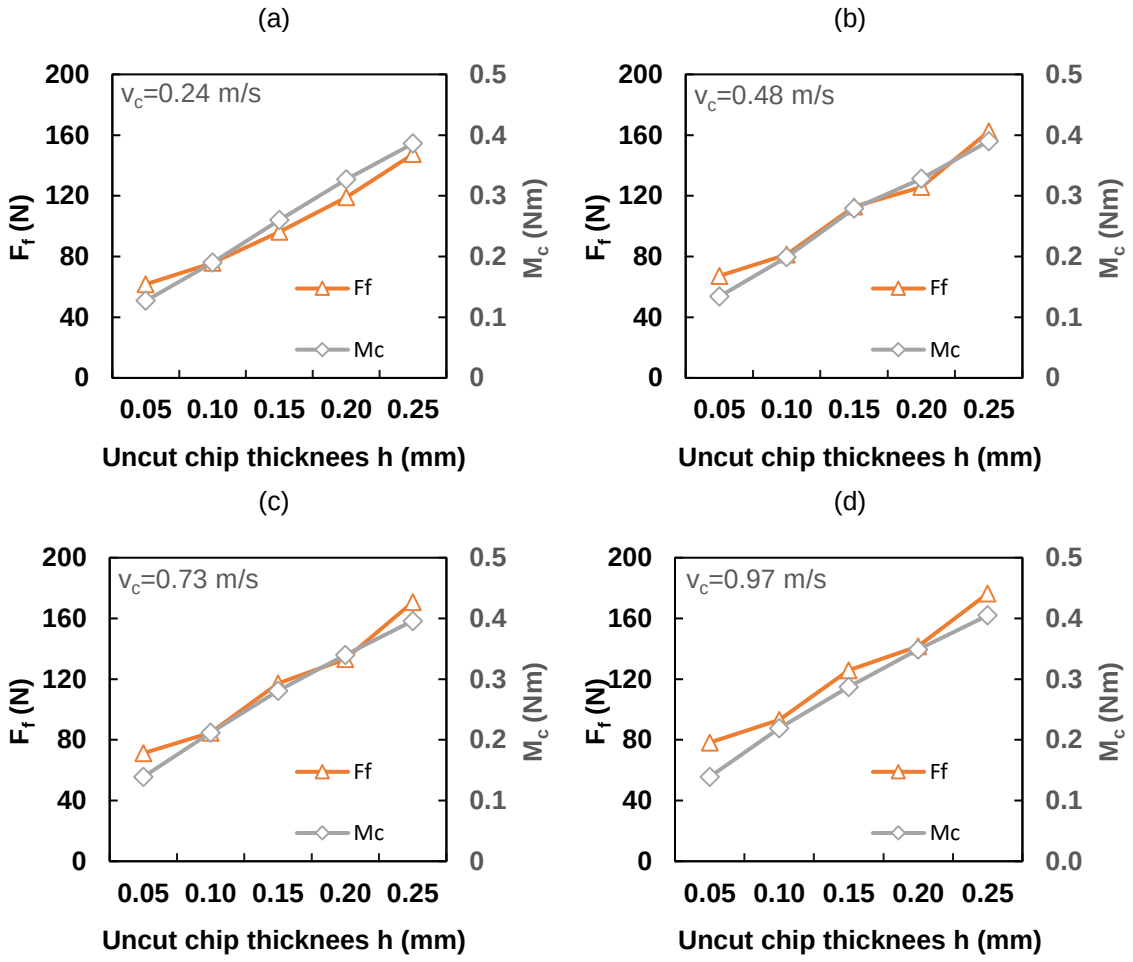

Fig. 6. Influence of uncut chip thickness on the value of thrust force and cutting moment for cutting speeds: (a) 0.24, (b) 0.48, (c) 0.73, and (d) 0.97 m/s.

The Process of Chip Formation

An important parameter of the machining process which characterises the amount of deformation in the shear zone is the shear angle ϕ (Fig. 7a) contained between the cutting speed direction and the shear surface. A smaller value indicates a greater shear zone length I_{sh} (Fig. 7b). The shear angle also affects the thickness of the chip (h_{ch}). The ratio of this thickness (h_{ch}) to the thickness of the machined layer (h) is called the cutting ratio (Λ_h), which is a measure of deformation in the shear zone, as shown in Eq. 2,

$$\Lambda_h = \frac{h_{ch}}{h} \quad (2)$$

where the h_{ch} is the thickness of the chip and h is thickness of the machined layer.

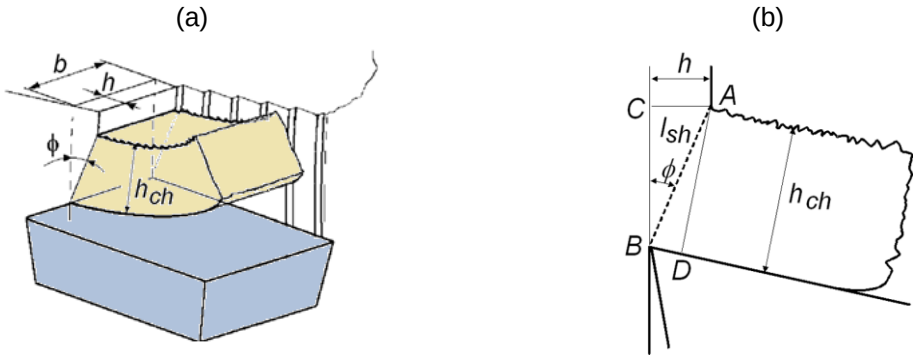

Fig. 7. (a) Shear angle and (b) cutting ratio

Table 2 shows the shape of chips obtained during the tests depending on the cutting parameters used. The chip thickness (h_{ch}) was measured using an optical microscope. Results of chip thickness are shown in Table 3. Figure 8 shows an example view of the chip thickness measuring method.

Table 2. Chip Shapes

v_c (m/s)	f_n = 0.1 (mm//rev)	f_n = 0.2 (mm/rev)	f_n = 0.3 (mm/rev)	f_n = 0.4 (mm/rev)	f_n = 0.5 (mm/rev)
0.24					
0.48					
0.73					
0.97					

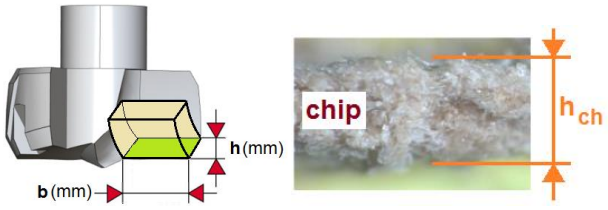

Fig. 8. Measurement of chip thickness

The cutting ratio (Λ_h) was used to determine the shear angle, as shown in Eqs. 3 through 7. The length of shear zone (l_{sh}) is the hypotenuse AB of two triangles: ABC and ABD (Fig. 7).

$$l_{sh} = \frac{h}{\sin\phi} = \frac{h_{ch}}{\cos(\phi - \gamma_o)} \quad (3)$$

$$\cos(\phi - \gamma_o) = \sin\phi\sin\gamma_o + \cos\phi\cos\gamma_o \quad (4)$$

$$\Lambda_h = \frac{h_{ch}}{h} = \sin\gamma_o + \frac{1}{tg\phi}\cos\gamma_o \quad (5)$$

$$tg\phi = \frac{\cos\gamma_o}{\Lambda_h - \sin\gamma_o} \quad (6)$$

where ϕ is the shear angle, γ_o is the tool rake angle, h_{ch} is the thickness of the chip, h is thickness of the machined layer and Λ_h is the cutting ratio.

Table 3. The Chip Thickness (h_{ch})

Cutting speed v_c (m/s)	Feed f_n (mm/rev)	Chip thickness h_{ch} (mm)
0.24	0.1	0.136
	0.2	0.245
	0.3	0.354
	0.4	0.431
	0.5	0.516
0.48	0.1	0.150
	0.2	0.262
	0.3	0.371
	0.4	0.445
	0.5	0.532
0.73	0.1	0.161
	0.2	0.273
	0.3	0.377
	0.4	0.462
	0.5	0.546
0.97	0.1	0.171
	0.2	0.280
	0.3	0.384
	0.4	0.475
	0.5	0.562

Figure 9 shows the variations of the shear angle in relation to the feed per tooth. The value of the feed per tooth and the cutting speed has a significant influence on the value of the shear angle. With the increase in the feed value, the value of the shear angle increased. However, the influence of the cutting speed on this angle demonstrated an inverse relationship. An increase in cutting speed caused a decrease in shear angle.

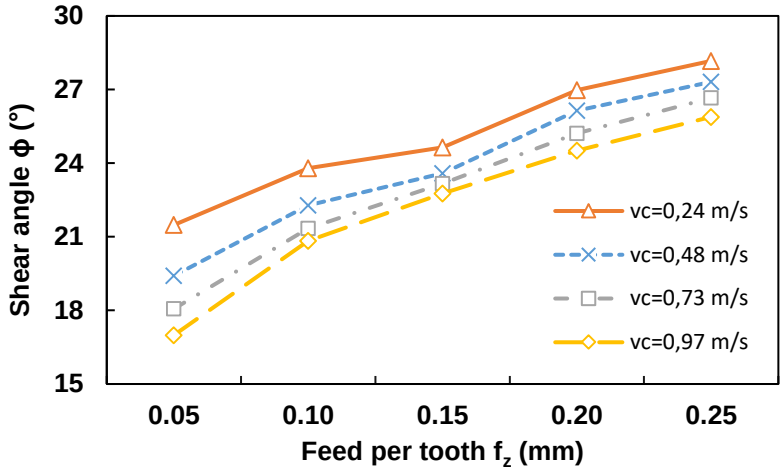

Fig. 9. The effect of the feed per tooth on shear angle

Forces in the Cutting Zone

Figure 10a shows the distribution of normal and contact stresses on the rake surface at free cutting (in the orthogonal plane). Normal stresses are biggest in the vicinity of the cutting edge and fall exponentially with distance from the edge. Tangential (contact) stresses are approximately the same along the zone of secondary shear and then decrease along the slip zone. They can be conventionally replaced by concentrated forces on the cutting edge: tangent to the rake face (F_γ) and normal to the rake face ($F_{\gamma N}$) as shown in Fig. 10b).

The resultant cutting force (F in Fig. 10b) acting on the drill blade can be divided into two components: horizontal (F_c) and perpendicular to the cutting edge in the orthogonal plane (F_o), as shown in Fig. 11. The component (F_o) can in turn be decomposed into two components, F_f and F_p. Thus, three components of the resulting cutting force may be obtained, F_f, F_p, and F_c. The cutting force (F_c) is the material's resistance force counteracting the rotation of the drill around its axis. This force results in the occurrence of cutting torque (M_c). The thrust force (F_f) is the resistance force of the material counteracting the drill's penetration. It works along the axis of the drill. If the force value for one blade is F_f, then the overall value will be $2F_f$ for both blades. Radial forces ($F_{p\,act}$) act on both opposite edges of the drill. These forces are balanced.

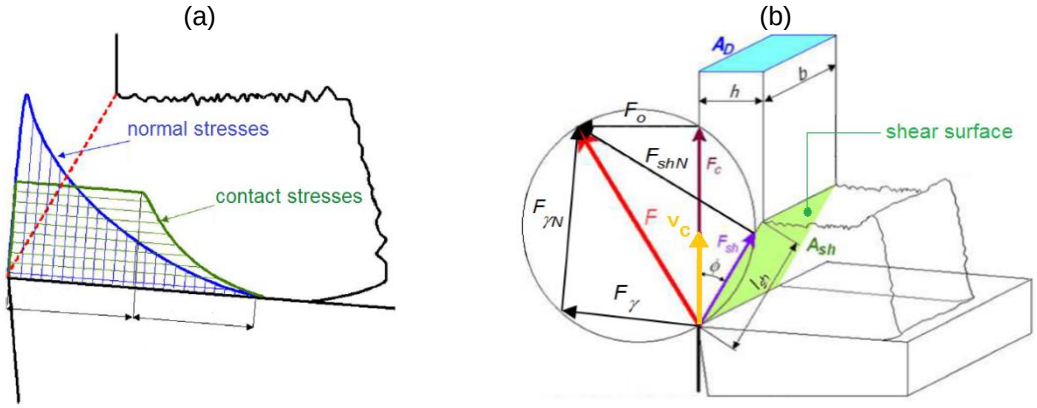

Fig. 10. Distribution of (a) stresses and (b) forces in the cutting zone

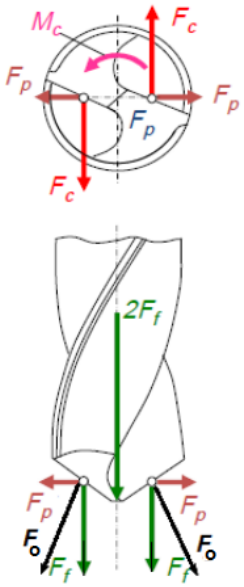

Fig. 11. Forces acting on cutting edge of drill

They are the components of the resultant cutting force (F). The impact of the tool on the chip is transferred on the shear surface, where both shear and normal stresses occur. These stresses, in turn, can be replaced by concentrated shear forces (tangent to shear surface) F_{sh} and normal to this surface F_{shN}. Of course, these forces also give a resultant cutting force (F). Analysing the effect of the tool on the workpiece in the tool-in-hand system, it is convenient to distribute the resultant cutting force (F) to the main cutting force (F_c) acting in the direction of the cutting speed as well as perpendicular to it and to the tangent plane the orthogonal force (F_o). Note that by plotting a circle whose diameter is the vector of the resulting cutting force, one can easily draw all three distributions of the discussed force (Fig. 10b).

It is particularly interesting to analyse the relationship of shear force (F_{sh}) as a function of shear area (Fig. 10b). This force is related to the forces acting in the tool-in-hand system by Eq. 7.

$$F_{sh}=F_c \cos\phi - F_o \sin\phi \quad (7)$$

By analysing the results of shear force (F_{sh}) measurements as a function of the shear area (A_{sh}), it can be seen that they are arranged along a straight line (Fig. 12).

The slope ratio of this straight line is known as shear resistance (k_{sh}), which in this case is equal to 12 N/mm^2. It changes very slightly in the range of cutting parameters examined. It can, therefore, be roughly regarded as a material constant. However, the line discussed (Fig. 12) does not originate from the beginning of the coordinate system. This indicates the presence of a component independent of the length of the shear area. This component is called the shearing force, which is applied to the cutting edge. Therefore, the shear force can be described by the relationship:

$$F_{sh}=F_{shk}+k_{sh}A_{sh} \quad (8)$$

where F_{shk} is the force acting on the active part of the cutting edge in a direction parallel to the shear plane (N).

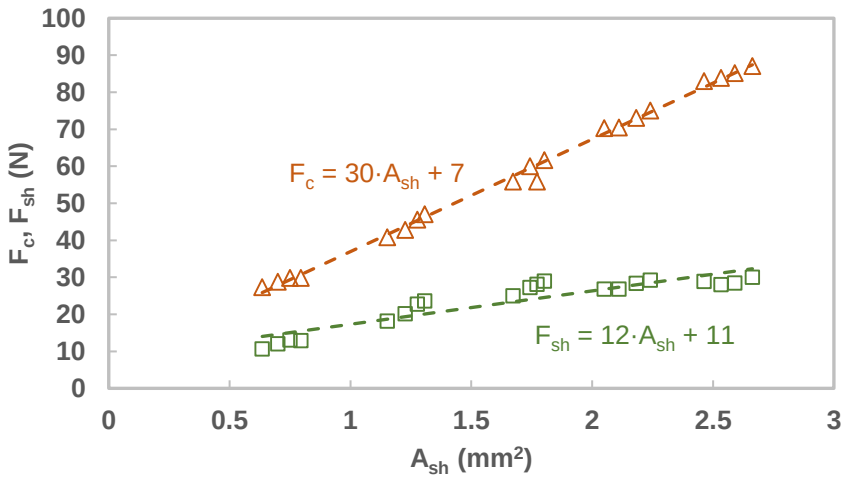

Fig. 12. Dependence of the main cutting force and shear force on shear area

Analogous equations can be presented for the main component of the cutting force (F_c),

$$F_c = F_{ck} + k_{shc} A_{sh} \quad (9)$$

where F_{ck} is the force acting on the active part of the cutting edge in the direction of the cutting speed (N), and k_{shc} represents the main shear resistance (slope ratio of this straight line F_c - A_{sh}), with units of N/mm^2.

It can be observed that the main shear resistance (k_{shc}), which in this case is 30 N/mm^2, is similar to the shear resistance (k_{sh}), the material constant. The ratio k_{shc}/k_{sh} is, therefore, also constant for a given workpiece and can be taken as a machinability index.

The area of the shear plane being the product of the width of the cutting layer (b) and the length of shear zone (l_{sh}) depends on the cross-sectional area of the cutting layer (thickness and width of this layer) and shear angle ϕ (Fig. 10b),

$$A_{sh} = b \cdot l_{sh} = b \cdot \frac{h}{\sin \phi} \quad (10)$$

Substituting (10) to (9) produces:

$$F_c = F_{ck} + \frac{A_D k_{shc}}{\sin \phi} \quad (11)$$

Thus, the cutting force depends on the dimensions of the cutting layer, the properties of the workpiece (which is quite obvious), and the shear angle.

While the k_{shc} values change to a relatively small extent with changes in the workpiece (similarly to the k_{sh}), the shear angle is very much dependent on the cutting conditions and affects the cutting force to a much greater extent than the shear resistance. The shear angle value increases with the increase of the cutting speed and the thickness of the machined layer, as shown schematically in Fig. 13. The shear angle in a great extent depends on force tangent to the rake face (F_γ). In turn, this force is a function of conditions of chip flow on the rake face as tool surface roughness of rake face and tool-chip contact length.

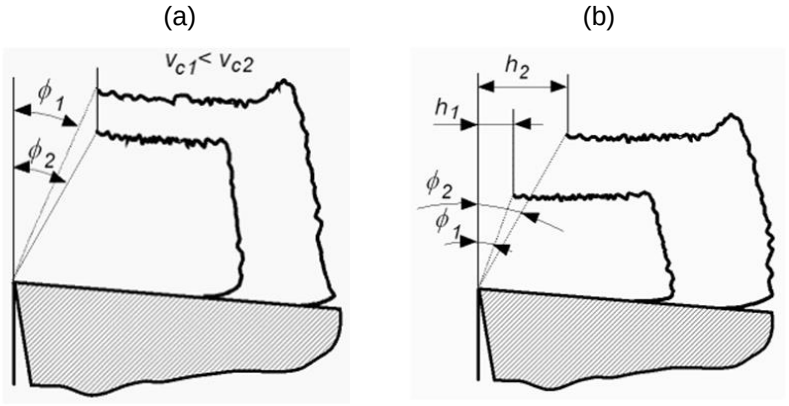

Fig. 13. Effect of (a) cutting speed and (b) chip thickness on the shear angle.

The values of shear resistance (k_{sh}) and the main shear resistance (k_{shc}) for the machining conditions analysed are listed in Table 4. The values of these parameters are slightly changed for a wide range of values of machining parameters. The ratio k_{shc}/k_{sh} is almost constant for a workpiece material and cutting parameters and can be used as a machinability index. However, the shear angle depends strongly on the cutting conditions and affects to a greater extent the cutting force value. Relation between the shear angle and cutting conditions is difficult to model.

Table 4. Machinability Index

Cutting speed v_c (m/s)	Feed f_n (mm/rev)	Cutting force F_c (N)	Shear force F_{sh} (N)	Shear resistance k_{sh} (MPa)	Main shear resistance k_{shc} (MPa)	Machinability index k_{shc}/k_{sh}
0.24	0.1	27.31	14.12	12.14	30.80	**2.537**
	0.2	40.86	24.14	12.14	30.80	**2.537**
	0.3	55.91	33.19	12.14	30.80	**2.537**
	0.4	70.32	35.71	12.14	30.80	**2.537**
	0.5	83.01	38.39	12.14	30.80	**2.537**
0.48	0.1	28.82	16.01	11.83	30.06	**2.541**
	0.2	42.80	26.86	11.83	30.06	**2.541**
	0.3	60.00	36.23	11.83	30.06	**2.541**
	0.4	70.54	35.62	11.83	30.06	**2.541**
	0.5	83.87	37.26	11.83	30.06	**2.541**
0.73	0.1	29.89	17.38	11.85	30.05	**2.536**
	0.2	45.59	30.22	11.85	30.05	**2.536**
	0.3	60.43	37.39	11.85	30.05	**2.536**
	0.4	73.12	37.78	11.85	30.05	**2.536**
	0.5	85.16	37.81	11.85	30.05	**2.536**
0.97	0.1	29.89	17.16	12.19	30.93	**2.537**
	0.2	47.10	31.42	12.19	30.93	**2.537**
	0.3	61.72	38.52	12.19	30.93	**2.537**
	0.4	75.05	38.88	12.19	30.93	**2.537**
	0.5	87.10	39.85	12.19	30.93	**2.537**

CONCLUSIONS

1. The feed rate has a significant influence on the value of the axial (thrust) force (F_f) and the cutting torque (M_c).
2. The value of the cutting force (F_c) in the MDF drilling process depends on the dimensions of the cutting layer, the properties of the workpiece, and the shear angle.
3. Both feed and cutting speed have a clear influence on the shear angle during the drilling process. An increase in the value of feed per tooth causes an increase in the shear angle, and an increase in the cutting speed reduces the shear angle.
4. The shear angle in a great extent depends on force tangent to the rake face. In turn, this force is a function of conditions of chip flow on the rake face as tool surface roughness of rake face and tool-chip contact length.

ACKNOWLEDGEMENTS

This research has been carried out with the use of research equipment purchased with help from the project "Establishment of the Intercollegiate Scientific and Research Laboratory in Stalowa Wola" under the Operational Program Development of Eastern Poland 2007-2013, Priority Axis I Modern Economy, Measure 1.3 Supporting Innovativeness pursuant to the contract No. POPW.01.03.00-18-016 / 12-00.

REFERENCES CITED

Aguilera, A., Meausoone, P. J., and Martin, P. (2000). "Wood material influence in routing operations: the MDF case," *Holz als Roh- und Werkstoff* 58(4), 278-283. DOI: 10.1007/s001070050425

Bhattacharyya, D., Allen, M. N., and Mander, S. J. (1993). "Cryogenic machining of Kevlar composites," *Mater. Manuf. Process.* 8(6), 631-652. DOI: 10.1080/10426919308934871

Chapman, K. M. (1998). "Composite panels in Australia and New Zealand: A focus on MDF," in: *Proceedings of the 32nd International Particleboard/Composite Materials Symposium* Pullman, WA, pp. 75-82.

Clark, P. A. (1991). "Panel products: past, present and future developments," *Journal of the Institute of Wood Science* 12, 233-241.

Costes, J., and Larricq, P. (2002). "Towards high cutting speed in wood milling," *Annals of Forest Science* 59(8), 857-865. DOI: 10.1051/forest:2002084

Davim, J. P., Clemente, V. C., and Silva, S. (2007). "Evaluation of delamination in drilling medium density fibre board,"*Proceedings of the Institution of Mechanical Engineers, Part B: Journal of Engineering Manufacture* 221(4), 655-658. DOI: 10.1243/09544054JEM781

Davim, J. P., Gaitonde, V. N., and Karnik, S. R. (2008). "An investigative study of delamination in drilling of medium density fibreboard (MDF) using response surface models," *International Journal of Advanced Manufacturing Technology* 37(1-2), 49-57. DOI: 10.1007/s00170-007-0937-8

Davim, J. P., and Reis, P. (2003). "Drilling carbon fiber reinforced plastics manufactured by autoclave-experimental and statistical study," *Materials Design* 24(5), 315-324. DOI: 10.1016/S0261-3069(03)00062-1

Dippon, J., Ren, H., Amara, F. B., and Altintas, Y. (2000). "Orthogonal cutting mechanics of medium density fibreboards," *Forest Products Journal* 50(7/8), 25-30.

Engin, S., Altintas, Y., and Amara, F. B. (2000). "Mechanics of routing medium density fiberboard," *Forest Products Journal* 50(9), 65-69.

EN 323 (1999). "Wood-based panels – Determination of density," European Committee for Standardization, Brussels, Belgium.

EN 322 (1999). "Wood-based panels – Determination of moisture content," European Committee for Standardization, Brussels, Belgium.

EN 310 (1994). "Wood-based panels: Determination of modulus of elasticity in bending and of bending strength," European Committee for Standardization, Brussels, Belgium.

EN 319 (1993). "Particleboards and fibreboards – Determination of tensile strength perpendicular to the plane of the board," European Committee for Standardization, Brussels, Belgium.

Feito, N., Díaz-Álvarez, J., Díaz-Álvarez, A., Cantero, J. L., and Miguélez, M. H. (2014). "Experimental analysis of the drill point angle and wear on the drilling of woven CFRPs," *Materials* 7(6), 4258-4271. DOI: 10.3390/ma7064258

Gaitonde, V. N., Karnik, S. R., and Davim, J. P. (2008a). "Prediction and minimization of delamination in drilling of medium-density fiberboard (MDF) using response surface methodology and Taguchi design," *Materials and Manufacturing Processes* 23(4), 377-384. DOI: 10.1080/10426910801938379

Gaitonde, V. N., Karnik, S. R., and Davim, J. P. (2008b). "Taguchi multiple-performance characteristics optimization in drilling of medium density fiberboard (MDF) to minimize delamination using utility concept," *Journal of Materials Processing Technology* 196(1-3), 73-78. DOI: 10.1016/j.jmatprotec.2007.05.003

Gordon, S., and Hillery, M. T. (2003). "A review of the cutting of composite materials," *Proceedings of the Institution of Mechanical Engineers, Part L: Journal of Materials: Design and Applications* 217(1), 35-45. DOI: 10.1177/146442070321700105

Irle, M., and Loxton, C. (1996). "Manufacture and use of panel products in the UK," *Journal of the Institute of Wood Science* 14(1), 21-26.

Ispas, M., Gurău, L., and Răcăşan. S. (2014). "Study regarding the variation of the thrust force, drilling torque and surface delamination with the feed per tooth and drill tip angle at drilling pre-laminated particleboard," *Pro Ligno* 10(4), 40-52.

Ispas, M., and Răcăşan, S. (2015). "The influence of the tool point angle and feed rate on the dynamic parameters at drilling coated particleboard," *Pro Ligno* 11(4), 457-463.

Ispas, M., and Răcăşan, S. (2017). "Study regarding the influence of the tool geometry and feed rate on the drilling quality of MDF panels," *Pro Ligno* 13(4), 174-180.

Jemielniak, K. (1998). *Machining*, Oficyna Wydawnicza Politechniki Warszawskiej, Warszawa. [in Polish].

Koch, K. (1964). *Wood Machining Processes*, Ronald Press, New York.

Lin, R. J. T., Van Houts, J., and Bhattacharyya, D. (2006). "Machinability investigation of medium-density fibreboard," *Holzforschung* 61(1), 71-77. DOI: 10.1515/HF.2006.013

Marchal, R., Mothe, F., Denaud, L., Thibaut, B., and Bleron, L. (2009). "Cutting forces in wood machining—Basics and applications in industrial processes," *Holzforschung*

63(2), 157-167. DOI: 10.1515/HF.2009.014
Palanikumar, K., Prakash, S., and Manoharan, N. (2009). "Experimental investigation and analysis on delamination in drilling of wood composite medium density fiber boards," *Materials and Manufacturing Processes* 24(12), 1341-1348. DOI: 10.1080/10426910902997100
Penman, D., Olsson, O. J., and Bowman, C. C. (1993). "Automatic inspection of reconstituted wood panels for surface defects," *Proceedings of the Society of Photo-Optical Instrumentation Engineers* 1823, 284-293.
Prakash, S., and Palanikumar, K. (2011). "Modeling for prediction of surface roughness in drilling MDF panels using response surface methodology," *Journal of Composite Materials* 45(16), 1639-1646. DOI: 10.1177/0021998310385026
Prakash, S., Palanikumar, K., and Manoharan, N. (2009). "Optimization of delamination factor in drilling medium-density fibre boards (MDF) using desirability-based approach," *International Journal of Advanced Manufacturing Technology* 45 (3-4), 370-381. DOI: 10.1007/s00170-009-1974-2
Sun, X., and Hammett, A. L. (1999). "Chinese furniture industry: Its development and wood use," *Forest Products Journal* 49(10), 31-35.
Szwajka, K., and Trzepieciński, T. (2016). "Effect of tool material on tool wear and delamination during machining of particleboard," *Journal of Wood Science* 62(4), 305-315. DOI: 10.1007/s10086-016-1555-6
Szwajka, K., and Trzepieciński, T. (2017). "An examination of the tool life and surface quality during drilling melamine faced chipboard," *Wood Research* 62(2), 307-318.
Szwajka, K., and Trzepieciński, T. (2017). "The influence of machining parameters and tool wear on the delamination process during milling of melamine-faced chipboard," *Drewno* 60(199), 117-131. DOI: 10.12841/wood.1644-3985.189.09
Valarmathi, T. N., and Palanikumar, K. (2011). "Evaluation of thrust force in drilling of medium density fiberboard (MDF) panels," *National Journal of Advances in Building Sciences and Mechanic* 2, 53-60.
Valarmathi, T. N., Palanikumar, K., and Latha, B. (2013a). "Measurement and analysis of thrust force in drilling of particle board (PB) composite panels," *Measurement* 46(3), 1220-1230. DOI: 10.1016/j.measurement.2012.11.024
Valarmathi, T. N., Palanikumar, K., and Sekar, S. (2013b). "Parametric analysis on delamination in drilling of wood composite panels," *Indian Journal of Science and Technology* 6(4), 4347-4356.
Valarmathi, T. N., Palanikumar, K., and Sekar, S. (2013c). "Thrust force studies in drilling of medium density fiberboard panels," *Advanced Materials Research* 622-623, 1285-1289. DOI: 10.4028/www.scientific.net/AMR.622-623.1285
Wyeth, D., Goli, G., and Atkins, A. (2009). "Fracture toughness, chip types and the mechanics of cutting wood," *Holzforschung* 63(2), 168-180. DOI: 10.1515/HF.2009.017

Article submitted: June 28, 2018; Peer review completed: August 25, 2018; Revised version received: September 12, 2018; Accepted: September 17, 2018; Published: September 20, 2018.
DOI: 10.15376/biores.13.4.8263-8278